

MINOTAUR: Multi-task Video Grounding From Multimodal Queries

Raghav Goyal^{*1,2} Effrosyni Mavroudi⁴ Xitong Yang⁴ Sainbayar Sukhbaatar⁴
 Leonid Sigal^{1,2,3} Matt Feiszli⁴ Lorenzo Torresani⁴ Du Tran⁴

¹University of British Columbia

²Vector Institute for AI

³CIFAR AI Chair

⁴Meta AI

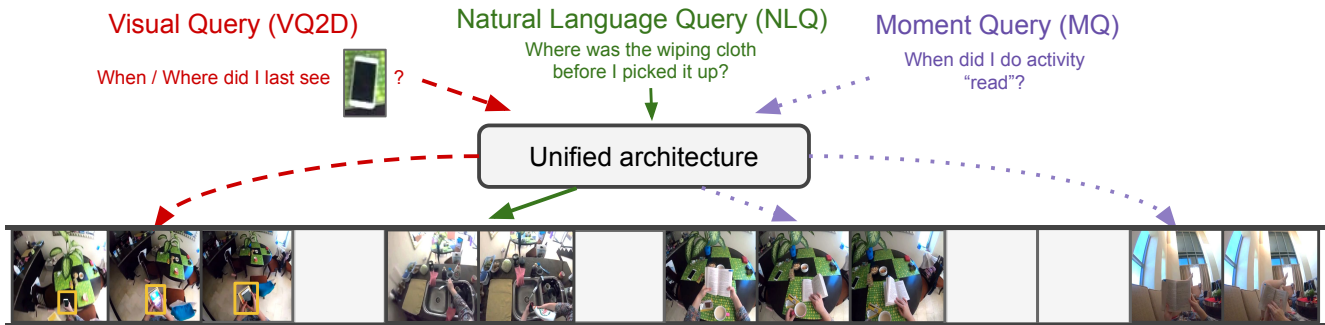


Figure 1. **Overview.** Our unified approach tackles the three episodic memory tasks with a single model architecture.

Abstract

Video understanding tasks take many forms, from action detection to visual query localization and spatio-temporal grounding of sentences. These tasks differ in the type of inputs (only video, or video-query pair where query is an image region or sentence) and outputs (temporal segments or spatio-temporal tubes). However, at their core they require the same fundamental understanding of the video, i.e., the actors and objects in it, their actions and interactions. So far these tasks have been tackled in isolation with individual, highly specialized architectures, which do not exploit the interplay between tasks. In contrast, in this paper, we present a single, unified model for tackling query-based video understanding in long-form videos. In particular, our model can address all three tasks of the Ego4D Episodic Memory benchmark which entail queries of three different forms: given an egocentric video and a visual, textual or activity query, the goal is to determine when and where the answer can be seen within the video. Our model design is inspired by recent query-based approaches to spatio-temporal grounding, and contains modality-specific query encoders and task-specific sliding window inference that allow multi-task training with diverse input modalities and different structured outputs. We exhaustively analyze relationships among the tasks and illustrate that cross-task learning leads to improved performance on each individual task, as well as the ability to generalize to unseen tasks,

such as zero-shot spatial localization of language queries.

1. Introduction

Video understanding aims to understand the events and objects captured in videos. This can facilitate users and agents (e.g., virtual assistants) to search for events of interest in massive video collections, enabling applications in augmented reality and robotics. For example, consider a virtual assistant that receives first-person footage of the activities of a user via a wearable device, as shown in Fig. 1, and can help the user remember where they left their phone or notify the user about the time they spent performing a particular activity, such as “reading”. These are examples of fine-grained video understanding tasks, which range from *activity detection* - finding the precise moments when an activity occurred in a video [4, 51, 73], to *temporal grounding* - finding the segments that are relevant to a natural language query [1, 6, 15, 29], or *visual query localization* - tracking a target object instance across a video [17].

Although researchers have been making consistent and significant advances in each one of these tasks by training individual, highly specialized models for each task using task-specific annotated datasets [4, 15, 18, 26, 47, 69],

* Work done during internship at Meta AI
 Correspondence: rgoyal14@cs.ubc.ca

there are two key limitations of state-of-the-art approaches that prevent them from being deployed in real-life applications such as AI assistants. First, designing and training **separate, single-task models** for each functionality not only requires storing multiple models, but it also fails to exploit the synergies between the tasks which could mutually benefit from each other. For example, a model that is able to understand language concepts (*e.g.* for temporal grounding of language queries) might be better able to detect activity classes by leveraging their semantic relationships encoded in their names, and vice versa, a model that can accurately detect activities can better reason about complex queries, such as “Where was the wiping cloth before I picked it up”. Furthermore, since annotating videos is time-consuming and costly, there typically exist small-to-medium scale datasets with annotations for a given task. Hence, training devoted, single-task, models limits the amount of training data that can be utilized. Second, most current state-of-the-art approaches are developed for **relatively short videos** (*e.g.*, spanning seconds to a couple of minutes), while real-life videos can span minutes to hours. Not only localizing answers to queries in such variable-length, long-form videos is a “needle-in-a-haystack” problem, but it breaks the assumptions of most models, *e.g.*, a single temporal segment being relevant to a language query [63].

In this paper, in an attempt to address these two limitations, we propose a unified, multi-task model for query-based video understanding. Our unified model can tackle multiple tasks during inference and can be trained with partially annotated data, *i.e.*, without requiring annotations for all tasks per video. Our key idea is to cast diverse tasks as special cases of spatio-temporal grounding of multi-modal queries. To further motivate this, let us take a closer look at the three video tasks shown in Fig. 1. A common theme that emerges is that the input consists of a long video and a query which can take the form of an image (cropped instance of the user’s mobile phone), an activity label of interest (such as “reading”), or a free-form natural language query, while the output is the temporal and/or the spatial extent of each relevant answer in the video.

Our unified model must localize both visual and textual queries at different granularity (*e.g.*, only temporally, or spatio-temporally). Designing such a model is challenging, as the type of input and output differs for each query. Our design is inspired by Transformer-based approaches, where the *trunk* of the architecture is occupied by a Transformer encoder-decoder framework [23, 40, 63], and task-specificity is baked into the input and output processing modules. Furthermore, we leverage parameter sharing and propose a simple training regime that is able to train a unified model using videos which have annotations for at least one of the tasks. Finally, to better handle long-form videos,

we design window-based training and inference regimes. That is, we train our model using fixed duration videos containing a single answer and then perform inference by applying the model in a sliding window fashion and appropriately fusing the predictions to retrieve all relevant answers to a query.

Contributions. In summary, the contributions of this work are three-fold. First, we propose MINOTAUR, a unified, Transformer-based model for grounding multi-modal queries in long-form videos. To the best of our knowledge, this is the first work that trains and evaluates a single model for tasks ranging from spatio-temporal grounding to activity detection. Second, we propose efficient, multi-task training and inference strategies, which enable training with fixed duration, partially annotated video segments, and testing on variable-length, long-form videos. Third, we train our model in both single-task and multi-task settings and evaluate it on the three tasks of the Ego4D Episodic Memory benchmark [17]: Visual Query 2D Localization (VQ2D), Moment Query localization (MQ), and Natural Language Query localization (NLQ). Our results show that our unified model outperforms or is on par with architectures that are designed and optimized for each individual task. Furthermore, multi-task training (optionally followed by single-task fine-tuning) leads to improved performance compared to single-task models.

2. Related Work

Visual Query (VQ2D) task. The output for the task is the most recent spatio-temporal localization of an input visual crop in a video. Recently proposed Siam-RCNN [17] uses a two-stage framework, where the first stage computes similarity between the visual crop feature and object-proposal features [48] across all images in a video, and retrieves the most similar object-proposal. In second stage, a KYS tracker [3] is initialized at the retrieved object-proposal and run in both forward and backward directions to get a contiguous spatio-temporal tube of the object. Xu *et al.* [62] takes this approach further and include background data to obtain a better performance. In contrast, our method uses a proposal-free, end-to-end encoder-decoder approach, and doesn’t rely on visual tracking.

Temporal video grounding. Temporal video grounding task involves retrieving or localizing temporal moments in a video that correspond to an input language query [6, 7, 19, 22, 35, 41, 49, 53, 58, 59, 68]. Prior works can be categorized into proposal-based approaches [1, 9, 15, 61, 67] where proposals are generated and ranked according to query, or proposal-free approaches [16, 66, 67] which directly predict the start and end positions. Recently, with the introduction of DETR [5], approaches such as Moment-DETR [29] have emerged which make use of set-based pre-

dictions. However, a limitation of the above approaches is that, in the case of long-videos, they rely on pre-extracted visual features to model long-temporal relations, but lack spatial information required for spatio-temporal detection.

Spatio-temporal video grounding. Spatio-temporal action detection requires localizing spatio-temporal tubes for all the actions in a video [24, 43, 56, 57, 60]. Prior works have approached the task from frame-level perspective [10, 43, 44, 50, 52, 60] where predictions are made on individual frames and linked to form action tubes, or tubelet-level perspective [21, 24, 30, 33, 64, 71] where they directly treat tubelet as a unit such as making 3D cuboid proposals.

Recent works, such as [63, 72], highlight the effectiveness of Transformer-based approaches for the task of detecting spatio-temporal tubes in videos. In particular, TubeR [72] proposed an end-to-end approach using no proposals or person detectors. On the other hand, TubeDETR [63] proposed a spatio-temporal grounding system, where the task is to localize spatio-temporal tube given a language query. We also use a Transformer-based approach, extending TubeDETR [63] to include task-specific components to enable multi-task learning and inference in long videos.

Vision and Language. Numerous approaches for handling vision and language tasks [8, 12, 14, 25, 27, 31, 32, 39, 54, 55] exist. However, they don’t translate well to spatio-temporal detection since they only focus on spatial data and localization. There also exists multi-modal approaches that fuse video-audio information [2, 37, 65], and in particular, UMT [37] takes into account audio signal in addition to video-text to perform Moment retrieval and highlight detection. Similarly, our approach accounts for multiple modalities in input except for audio, but for output we make more granular spatio-temporal predictions over long videos.

Multi-task learning. Recent works have explored multi-task learning at the intersection of vision and language [40, 42, 46]. In particular, Lu *et al.* [40] trains on 12 tasks with task-specific prediction heads, hyper-parameters and training schedule. In our work, we also use task-specific components for encoding query and decoding outputs, however, we make use of a single set of hyper-parameters and training schedule, as we have lower number of tasks (*i.e.* 3).

3. Approach

Our goal is to tackle a family of *episodic memory* tasks, *i.e.*, tasks that query a user’s experience in the past, as it is captured in an egocentric video recorded by a wearable camera. Depending on the type of query, the tasks are categorized as: (1) Visual Query (VQ2D), in which given an image of an object as query and a video, the output is a spatio-temporal tube of the most recent occurrence of the object in the video; (2) Natural Language Query (NLQ),

in which given a textual query and a video, the output is a temporal extent where the answer can be found; and (3) Moment Query (MQ), in which given a query in the form of an activity name and a video, the output is all the temporal extents where the activity occurs.

Instead of designing and training separate, dedicated models for each of these diverse tasks, we leverage their inherent similarities to propose a *unified model that can localize any type of query (visual, textual or categorical) in long-form egocentric videos*. This is desirable since it paves the way for a holistic video understanding system that can reason across space-and-time about objects and actions.

3.1. Problem Formulation

Formally, the three episodic memory tasks can be described as follows: given an egocentric video \mathcal{V} and a query \mathcal{Q}_ν , the goal is to identify a response track \mathcal{R}_ν , where $\nu \in \{\text{VQ2D}, \text{NLQ}, \text{MQ}\}$. Specifically,

- **VQ2D.** With Query \mathcal{Q}_ν as a visual crop of an object, the response track is a temporally contiguous set of bounding boxes, *i.e.*, a spatio-temporal tube tracking the object of interest, $\mathcal{R}_\nu = \{r_s, r_{s+1}, \dots, r_e\}$, where s and e are start and end frame indices respectively, and r_i is a bounding box $(x, y, w, h) \in \mathbb{R}^4$ in i^{th} frame. If there are multiple occurrences of the object, the most recent occurrence before the query frame is retrieved.
- **NLQ.** With Query \mathcal{Q}_ν as a text question, the response track is a temporally contiguous set of frames or a temporal extent, $\mathcal{R}_\nu = [s, e]$, where s and e are start and end frame indices, respectively.
- **MQ.** With Query \mathcal{Q}_ν being an activity, or templated question about activity c (*e.g.*, “When did I do c ?”), the response consists of all the instances of activity c in the video, $\mathcal{R}_\nu = \{(s_n, e_n, g_n)\}_{n=1}^N$, where N is the total number of instances, s_n and e_n are start and end frame indices for the n^{th} instance and g_n is the confidence.

3.2. Unified approach for Multi-task Video Grounding of Multimodal Queries

To jointly solve these three episodic memory tasks with a unified model, we introduce MINOTAUR, a Transformer-based architecture, illustrated in Figure 2. Our model receives an egocentric video and a query (visual, textual, or categorical) as inputs, and encodes them with a *Visual Backbone* and a *Modality-Specific Query Encoder*, respectively. After obtaining the video and query features, they are fused with a *Video-Query Encoder* that captures multi-modal interactions. Then, the context-aware video-query features are decoded using a *Space-Time Decoder*, which models long-range temporal interactions. The decoded features are fed to *prediction heads* to generate a bounding box prediction, as well as predictions for the start, end, and foreground

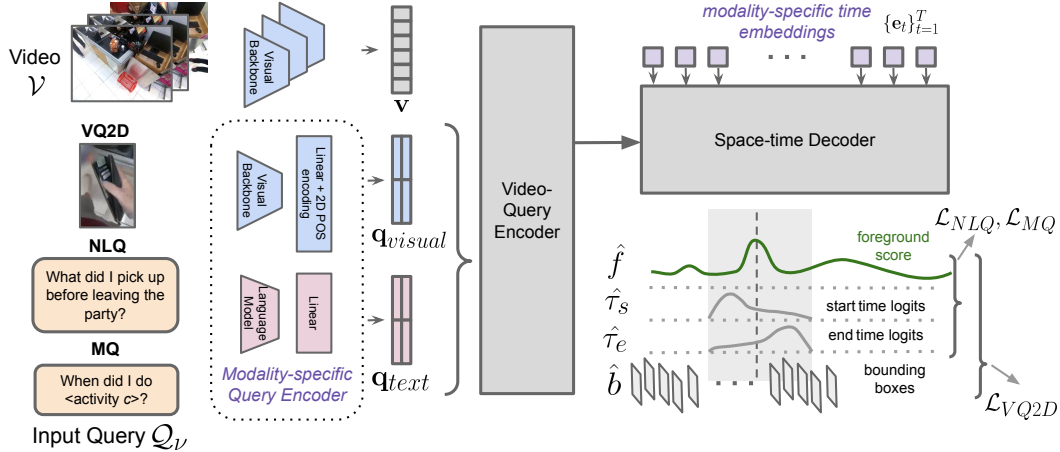


Figure 2. **Overview of the model** Given a video \mathcal{V} and task-query Q_ν , our model encodes them using a Visual Backbone and Modality-specific Query Encoder. The obtained video and query features, \mathbf{v} and \mathbf{q} , are encoded by Video-Query Encoder and decoded using Space-time Decoder by refining Modality-specific time embeddings $\{\mathbf{e}_t\}_{t=1}^T$. Finally, the prediction heads predict foreground, start/end time logit, and bounding box for every frame.

probabilities at each video frame index. Lastly, these predictions are processed by *task-specific output processing* modules, which convert them to the desired response track \mathcal{R}_ν for each task.

We base our architecture on TubeDETR [63], a state-of-the-art architecture for spatio-temporal grounding of natural language queries. Our model generalizes TubeDETR to handle multiple input query modalities, together with task-specific outputs in a long-form video, where the outputs can take the form of a single or multiple instances of spatio-temporal or temporal tubes. We describe TubeDETR [63] below and our task-specific components in Section 3.2.1.

Visual backbone. We start with encoding T frames of video \mathcal{V} using a 2D-CNN backbone and a feed-forward layer. We add 2D positional encoding to the features and flatten them to give $\mathbf{v} \in \mathbb{R}^{T \times HW \times d}$, where T is the number of frames, H and W are height and width of feature map and d is the hidden size of the model.

Video-Query encoder. Given input query features $\mathbf{q} \in \mathbb{R}^{L \times d}$ from our Modality-specific Query Encoder (described later in Section 3.2.1), where d is the hidden size of the model and L is the size of the query features, we replicate \mathbf{q} across T frames, concatenate with video features \mathbf{v} , and forward it through a N_e -layer transformer encoder to give $Enc(\mathbf{v}, \mathbf{q}) \in \mathbb{R}^{T \times (HW+L) \times d}$. The encoder applies transformer layers to each frame-query feature independently and effectively fuses query information with every frame feature. Note that for computational reasons, the video-query encoder can be applied to downsampled video-query features (sampled at regular intervals with stride k) and the output can be temporally replicated or upsampled by the factor of k to match the original T number of frames.

Space-time decoder. The decoder takes as input a sequence of T learned, modality-specific time embeddings $\{\mathbf{e}_t\}_{t=1}^T \in \mathbb{R}^d$ (described later in Section 3.2.1). The decoder then refines the time embeddings for each frame t by cross-attending to video-query encoder features $Enc(\mathbf{v}, \mathbf{q})$ in order to predict whether the answer to the query is visible at each frame t . Following TubeDETR [63], decoding is factorized over time and space for efficiency by having N_d -blocks of temporal self-attention and frame-wise cross-attention layers, interleaved with feed-forward and normalization layers. The temporal self-attention layer allows time embeddings to attend to each other, thereby facilitating temporal interactions across the video. The frame-wise cross-attention layer performs cross-attention on each frame separately, where for an t^{th} frame, the corresponding time embedding \mathbf{e}_t cross-attends to its video-query encoder feature $Enc(\mathbf{v}, \mathbf{q})_i \in \mathbb{R}^{(HW+L) \times d}$. In effect, the decoder accounts for information in both temporal and spatial dimensions to produce refined time embeddings. See [63] for more details. Finally, the refined time embeddings $\{\hat{\mathbf{e}}_t\}_{t=1}^T$ are used for making predictions for every frame in the video.

3.2.1 Modality-specific Encoders and Inference

In this section, we describe the novel components of our architecture, inference procedures and losses that enable us to train and employ a single, unified model for all tasks.

Modality-specific query encoder. Depending on the task, the query Q_ν can be a text question in the case of MQ and NLQ, or a visual crop in the form of image in the case of VQ2D. To handle different query modalities, we introduce a modality-specific query encoder. Language queries are embedded using a RoBERTa language model

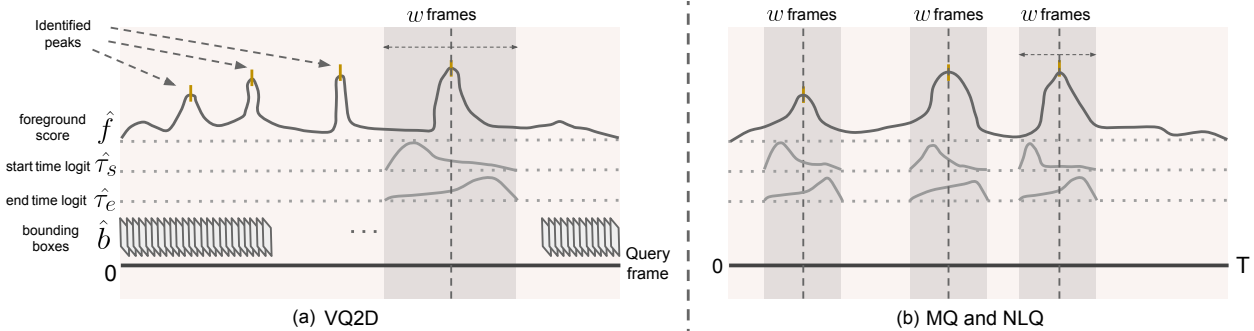


Figure 3. **Task-specific inference.** During inference, we identify all possible peaks from the time-series of foreground scores \hat{f} , and for generating VQ2D predictions (a), we retrieve the most recent occurrence of an object by forming predictions around the latest peak, while for MQ and NLQ (b), we use all the peaks for generating temporal segments and rank them according to their respective heights.

and mapped to hidden size d of the model using a feed-forward layer, $\mathbf{q}_{text} \in \mathbb{R}^{L' \times d}$, where L' is the number of tokens. On the other hand, visual queries are encoded using the visual backbone and a feed-forward layer. The resulting features are flattened along spatial dimensions to give $\mathbf{q}_{visual} \in \mathbb{R}^{H'W' \times d}$, where H' , W' are spatial dimensions of the feature map. Formally, the query feature can be written as $\mathbf{q} \in \mathbb{R}^{L \times d}$, where $L \in \{L', H'W'\}$.

Modality-specific time embeddings. As described earlier, the Space-time decoder takes as input a sequence of time embeddings $\{\mathbf{e}_t\}_{t=1}^T$ and refines them using the encoded video-query features. We obtain the above modality-specific time embeddings by replicating a learned, modality-specific encoding vector (\mathbf{e}^{text} or \mathbf{e}^{visual}) across time T and summing it with a sinusoidal time-encoding.

Prediction heads. Similar to TubeDETR [63], we use MLPs to predict for each frame t : (a) the relative coordinates for the bounding box $\hat{\mathbf{b}}_t \in [0, 1]^4$ related to the query, (b) the score $\hat{\tau}_{s,t}$ that frame t is the start of an answer to the query, and (c) the score $\hat{\tau}_{e,t}$ that frame t is the end of an answer. To better handle long-form videos, where multiple segments can be relevant to the query, we also output a confidence score \hat{f}_t for each frame being relevant to the query. In summary, our model outputs 7-dimensional vector, $[\hat{\mathbf{b}}, \hat{\tau}_s, \hat{\tau}_e, \hat{\mathbf{f}}] \in \mathbb{R}^{T \times 7}$, as predictions for every frame in the video (shown in Fig 3 (a)).

Task-specific inference. Due to the limitations of GPU memory our model cannot process all frames of a long-form video at once. To handle that, we adopt a sliding window approach, where we train using video segments of fixed duration of w frames, and perform inference by aggregating model outputs in a sliding window fashion. These outputs then need to be post-processed to generate task-appropriate response tracks. To predict a spatio-temporal tube, we form probabilities for start and end time, $\hat{\mathbf{p}}_s$ and $\hat{\mathbf{p}}_e$ by taking softmax over the logits $\hat{\tau}_s$ and $\hat{\tau}_e$ respectively. We infer start and end frame indices, \hat{s} and \hat{e} , by choosing argmax

over the distributions such that $\hat{e} > \hat{s}$. The spatial predictions are formed by selecting bounding boxes in the predicted start/end range, resulting in space-time tube $\{\hat{\mathbf{b}}_t\}_{t=\hat{s}}^{\hat{e}}$.

Inference: VQ2D. The task requires finding the most recent occurrence of a query object. Therefore, we use foreground scores $\hat{\mathbf{f}} \in \mathbb{R}^T$ to identify a set of peaks in the scores which would indicate high probability of occurrence. From the set of peaks, we select the most recent one as our candidate peak as shown in Fig 3(a). We sample a window of size w frames around the peak, and predict start and end frame indices, \hat{s} and \hat{e} , by only considering the predictions within the window, *i.e.*, outside the selected window, the start and end time probabilities, \hat{p}_s and \hat{p}_e , are zero.

Inference: NLQ + MQ. Since the two tasks require multiple predictions, we generate predictions using all identified peaks, and sort the predictions using the scores of the peaks. In addition NLQ and MQ don't require bounding boxes, so we only predict time intervals (or frame indices).

Training. During training, we randomly sample a window of w frames (out of total T frames) around a ground-truth temporal segment that answers the query (if there are multiple ground-truth segments we randomly pick one). In the case that the ground-truth segment is longer than w , we randomly place the window covering a part of the ground-truth.

Losses. Our model is trained using *spatial losses*, which refine the bounding box predictions, and *temporal losses*, which refine the start/end/foreground frame predictions). In particular, given ground-truth bounding boxes $\mathbf{b} \in [0, 1]^{4 \times (e-s+1)}$ for every frame between the ground-truth start frame s , and end frame e , the spatial loss computes \mathcal{L}_1 and generalized IoU (\mathcal{L}_{gIoU}) [5] loss between \mathbf{b} and $\hat{\mathbf{b}}$ as:

$$\mathcal{L}_{spatial} = \lambda_{\mathcal{L}_1} \mathcal{L}_{\mathcal{L}_1}(\hat{\mathbf{b}}, \mathbf{b}) + \lambda_{gIoU} \mathcal{L}_{gIoU}(\hat{\mathbf{b}}, \mathbf{b}). \quad (1)$$

For temporal losses, we define target start and end time distributions ($\mathbf{p}_s, \mathbf{p}_e \in [0, 1]^w$) using standard Normal ($\mathcal{N}(\cdot, 1)$) centered at the ground-truth start and end frames,

respectively. For predicted start and end time logits ($\hat{\tau}_s, \hat{\tau}_e \in \mathbb{R}^w$), we normalize them across w frames using softmax to get corresponding probabilities ($\hat{\mathbf{p}}_s, \hat{\mathbf{p}}_e \in [0, 1]^w$), and compute KL-divergence (\mathcal{L}_{KL}) between target distribution \mathbf{p}_s (or \mathbf{p}_e) and predicted distribution $\hat{\mathbf{p}}_s$ (or $\hat{\mathbf{p}}_e$). In addition, we also regress foreground scores, $\hat{\mathbf{f}} \in [0, 1]^w$, which indicate the likelihood of a frame to be a part of the ground-truth. We form our target as $\mathbf{f} \in \{0, 1\}^w$, such that \mathbf{p} is 1 within the start and end frame indices (s and e), and 0 otherwise. We use positive-weighted binary cross-entropy loss (\mathcal{L}_{BCE}) between \mathbf{f} and $\hat{\mathbf{f}}$ to compute foreground loss. Lastly, we have guided attention loss $\mathcal{L}_{att}(A)$ which promotes cross-attention weights in space-time decoder to be diagonal-like and have greater values in their corresponding temporal boundaries (see [63]).

$$\begin{aligned} \mathcal{L}_{temporal} = & \lambda_{KL} [\mathcal{L}_{KL}(\hat{\mathbf{p}}_s, \mathbf{p}_s) + \mathcal{L}_{KL}(\hat{\mathbf{p}}_e, \mathbf{p}_e)] \\ & + \lambda_f \mathcal{L}_{BCE}(\hat{\mathbf{f}}, \mathbf{f}) + \lambda_{att} \mathcal{L}_{att}(A) \end{aligned} \quad (2)$$

Depending on the type of ground-truth annotations that are available for each task, the model is trained with different loss components. Since, NLQ and MQ only have temporal annotations, we employ only the *temporal* loss terms: $\mathcal{L}_{NLQ} = \mathcal{L}_{MQ} = \mathcal{L}_{temporal}$. However, for VQ2D where we have ground-truth spatio-temporal tubes available, we apply all loss terms: $\mathcal{L}_{VQ2D} = \mathcal{L}_{spatial} + \mathcal{L}_{temporal}$.

3.2.2 Multi-Task Learning

One benefit of accommodating the three Episodic Memory tasks into a single, unified architecture, is the potential for mutual beneficial cross-transfer of knowledge among the tasks. We experimentally explore all joint and transfer combinations. For joint-training we use Round-Robin Batch-Level Sampling which has been found to be effective in multi-task training [40]. The sampling scheme samples batches from tasks one-by-one in a cyclical manner, effectively training the model with equal proportion of individual tasks even though the dataset sizes of the tasks could be different. The total loss in multi-task learning is the sum of the individual tasks’ losses.

4. Experiments

Datasets. Ego4D is a large-scale egocentric video dataset which is accompanied by benchmarks that evaluate first-person visual understanding [17]. We experiment with the three tasks of the Episodic Memory benchmark and use the official data splits for each task [17]. **VQ2D** consists of roughly 22k video-query pairs spread over 6k video clips. The dataset is divided into train, val and test sets with 13.6k, 4.5k and 4.4k video-query pairs. The mean length of spatio-temporal tubes is approx. 15 frames (3 secs). The most frequent video length on which the visual search is performed during evaluation is 1.5k frames (5 mins), with

maximum up to approx. 4.5k frames (15 mins). **NLQ** consists of 19.2k video-query pairs divided into train, val and test set with ratio 3:1:1. Language queries are based on 13 query templates involving objects, events, places and people. The mean and mode of temporal tube length in train set is approx. 54 (11 secs) and 6 (1.2 sec) frames respectively. The most frequent video length on which the visual search is performed during evaluation is 8 mins, with maximum up to 20 mins. **MQ** has 22.2k action instances across 2.5k videos with 110 activity classes. The dataset is divided into train, val and test sets with 3:1:1 ratio. The mean and mode of temporal tube length in train set is approx. 220 (44 secs) and 7 (1.4 sec) frames respectively. The most frequent, and also maximum, video length on which the visual search is performed during evaluation is 8 mins.

Evaluation metrics. For each task, we use the evaluation metrics defined in Ego4D [17]. For **VQ2D** we report the *temporal AP* (tAP₂₅) and *spatio-temporal AP* (stAP₂₅) which measure the average-precision of predicted temporal and spatio-temporal extent of a tube with the ground-truth at an IoU threshold of 0.25. We also have *Recovery* (rec%) which calculates % of frames in predicted tube where bounding box has at least 0.5 IoU with the ground-truth, and lastly we have *Success* (Succ) which measures whether prediction has any overlap with ground-truth as % of samples where prediction has at least 0.05 IoU with the ground-truth. **NLQ** is evaluated using *recall@k, tIoU=m*, with $k \in \{1, 5\}$ and $m \in \{0.3, 0.5\}$, which measures the percentage of samples where at least one of the top- k predictions has temporal IoU of at least m with the ground-truth. For **MQ**, we have *recall@kx, tIoU=m*, with $k \in \{1, 5\}$ and $m \in \{0.3, 0.5\}$, which measures % of predicted instances of class x that have at least one prediction with tIoU greater than m in the top- k results.

Implementation details. Following TubeDETR [63], we use a ResNet-101 [20] as our visual backbone and RoBERTa [38] as the language model. We pre-process videos by resizing them with a shorter side size of 320, and sampling them at 5 fps. During training, we sample a window of length w , where w is 200, 400 and 400 frames, decoded at 5, 1 and 1 fps, and downsampled with stride 1, 5 and 5 for VQ2D, NLQ and MQ, respectively. The rest of our hyperparameters are adopted from TubeDETR [63]: $N_e = N_d = 6, d = 256, \lambda_{\mathcal{L}_1} = 5, \lambda_{\mathcal{L}_{gIoU}} = 2, \lambda_{KL} = 10, \lambda_{att} = 1, \lambda_f = 2$. We initialize our weights from MDETR [25] which is pretrained on Flickr30K [45], MS COCO [11] and Visual Genome [28]. We train our models on 16 Quadro GV100 GPUs with an effective batch size of 16 videos for 25 epochs with a drop in learning rate at every 10th epoch by a factor of 10. The final model is selected based on best performance on a small subset of validation data.

		VQ2D				NLQ				MQ				# params (# models)	
		tAP ₂₅	stAP ₂₅	rec%	Succ	tIoU=0.3		tIoU=0.5		tIoU=0.3		tIoU=0.5			
						R@1	R@5	R@1	R@5	R@1x	R@5x	R@1x	R@5x		
Joint	1	Ego4D [17]	0.20	0.12	32.2	39.8	5.45	10.74	3.12	6.63	33.45	58.43	25.16	46.18	432M (3)
	2	Single-Task	0.41	0.21	29.4	61.2	6.53	17.22	3.61	9.58	33.64	55.38	23.86	39.48	
	3	All-Tasks (AT)	0.41	0.19	26.4	60.2	7.74	21.14	4.78	12.60	34.82	56.68	25.58	42.30	
Transfer	4	NLQ → MQ	-	-	-	-	-	-	-	-	32.70	55.17	23.67	40.78	185M (1)
	5	VQ2D → MQ	-	-	-	-	-	-	-	-	35.75	56.17	26.05	41.78	
	6	MQ → NLQ	-	-	-	-	6.94	19.93	4.13	11.72	-	-	-	-	185M (1)
	7	VQ2D → NLQ	-	-	-	-	6.69	17.73	4.26	10.66	-	-	-	-	
	8	MQ → VQ2D	0.40	0.21	29.1	60.4	-	-	-	-	-	-	-	-	61M (1)
	9	NLQ → VQ2D	0.42	0.20	29.2	61.1	-	-	-	-	-	-	-	-	
	10	AT → Tasks	0.42	0.22	29.4	61.1	7.69	21.17	5.21	12.98	33.82	56.61	25.21	42.83	185M (1)

Table 1. **Multi-task and transfer learning on validation set.** We observe that, 1) our All-Tasks (AT) model trained using multi-task learning outperforms individual Single-Task models, and 2) further fine-tuning AT to individual tasks typically lead to better performance.

4.1. Single-task and Multi-task Learning

Single-Task v/s Multi-Task Performance. We train our model individually on the three tasks to setup a baseline for multi-task learning, Single-Task, see row 2 of Table 1. We use the same model architecture except in the case of VQ2D where text encoder is not needed. We train a single model, All-Tasks (AT), on all the three tasks with results shown in row 3. We observe that the All-Tasks (AT) model outperforms Single-Task models on NLQ and MQ across all the metrics. However, we see a slight decrease in 3 out of 4 metrics in the case of VQ2D, which could be attributed to joint training collectively optimizing for tasks where two of the tasks are temporal-only (NLQ and MQ) and one spatio-temporal task (VQ2D). Moreover, the total number of models required for all three tasks drops from 3 to 1, and the total number of parameters drops by a factor of 2.3×.

Transfer learning. We also explore pair-wise transfer between the tasks where a model trained on one task is used as an initialization for the other task, shown in rows 4 - 9. We observe that the transfer outperforms Single-Task performance in 4 out of 6 cases. For **MQ** (rows 4 - 5), we observe better transfer performance from VQ2D compared to NLQ. One possible explanation is that the queries in MQ are from a set of 130 activity templates in the form of “When did I do *activity c*?”, so its reliance on text encoder is low and sees more gain in performance from the visual task than its language counterpart.

Multi-Task learning as pre-training. Following Lu *et al.* [40], we also experiment with transferring All-Tasks (AT) model to individual tasks with the idea that AT model may allow downstream tasks to take advantage from multi-task training. The results are shown in row 10. Across the three tasks, we observe better performance than Single-

Task, which indicates effectiveness of multi-task training.

4.2. Comparison with Existing Work

We compare our All-Tasks (AT) model to the prior works in Table 2. Compared to the Ego4D [17] baselines, we outperform on 9 out of total 12 metrics across the three tasks despite the fact that the Ego4D [17] baselines are three dedicated, task-specific architectures. In contrast, our approach uses a single architecture, with similar input data pipeline and inference procedure, and is positioned to train and benefit across multiple tasks.

We also highlight the winners of task-specific challenge hosted in CVPR’22 workshop [13]. Specifically, Xu *et al.* [62] extends the VQ2D baseline and augmented data with background frames. ReLER@ZJU [36] proposed a multi-scale transformer along with an extensive augmentation routine involving variable-length sliding windows, video splicing and contrastive losses. Finally they use an ensemble of models trained in SlowFast and Omnivore features for their challenge entry. Lastly, EgoVLP [34] follows the same architectures as the Ego4D baselines, but uses features pretrained on a much larger 3.8M video-text pairs from Ego4D [17] using contrastive learning. At the time of writing, there is a second round of challenge hosted in ECCV’22 workshop but we do not have the final technical reports of the submitted entries to make any meaningful comparison.

4.3. Qualitative Results

We show a few examples of spatio-temporal predictions on NLQ task using All-Tasks model in Figure 4. We observe that even though the spatial branch of the model was trained only on VQ2D data, it makes non-trivial *zero-shot* spatial localization for the language queries.

	Methods	VQ2D				NLQ				MQ			
		tAP ₂₅	stAP ₂₅	rec%	Succ	tIoU=0.3		tIoU=0.5		tIoU=0.3		tIoU=0.5	
						R@1	R@5	R@1	R@5	R@1x	R@5x	R@1x	R@5x
Ego4D [17]	Siam-RCNN [17]	0.21	0.13	34.0	41.6	-	-	-	-	-	-	-	-
	VSLNet [67]	-	-	-	-	5.47	11.21	2.80	6.57	-	-	-	-
	VSGN [70]	-	-	-	-	-	-	-	-	33.56	59.79	24.25	46.22
Ours	All-Tasks (AT)	0.41	0.19	26.5	60.6	7.47	19.61	4.85	12.09	35.10	56.63	24.62	41.27
	AT → Tasks	0.42	0.21	29.0	61.4	8.07	20.63	5.52	12.94	34.27	56.45	24.44	41.39
CVPR'22 Workshop [13]	Xu <i>et al.</i> [62]	0.24	0.17	37.2	45.1	-	-	-	-	-	-	-	-
	ReLER@ZJU [36]	-	-	-	-	12.89	15.41	8.14	9.94	-	-	-	-
	EgoVLP: VSLNet* [34]	-	-	-	-	10.46*	16.76*	6.24*	11.29*	-	-	-	-
	EgoVLP: VSGN* [34]	-	-	-	-	-	-	-	-	-	-	28.03*	-

Table 2. **Comparison with existing work on test set.** We outperform on 9 out of total 12 metrics compared to the Ego4D [17] baselines across the three tasks despite the fact that they are three dedicated, task-specific architectures. (The rows in grey denote unpublished works at the time of writing and the entries with asterisk (*) use additional data)

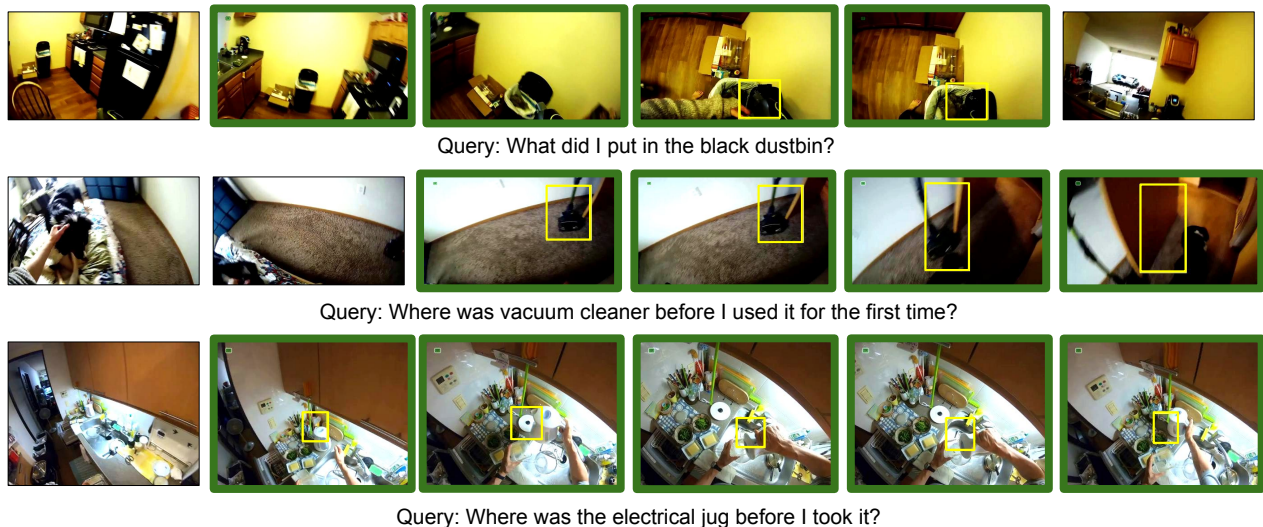


Figure 4. **Spatio-temporal predictions for NLQ with the All-Tasks (AT) model.** Predictions are shown with yellow bounding boxes, while ground-truth temporal segments are denoted with green borders. Although the model has not been trained with ground-truth spatio-temporal tubes for language queries, multi-task training results in some meaningful results for zero-shot spatio-temporal grounding.

4.4. Ablation

Batch-level sampling: Round-Robin v/s Concat. In multi-task training, we can combine different tasks, by either concatenating the datasets together (*Concat*), or we can sample batches in *Round-Robin* fashion such that each dataset is sampled equally even though the individual dataset sizes are skewed. As shown in Table 4 in Ablation B, we found that *Round-Robin* performs better on average.

Peak-based predictions. Making predictions on long videos is challenging when we are tasked with predicting spatio-temporal regions of interest with short temporal extents compared to the whole video. As detailed previously, we approach this by identifying peaks in foreground scores \hat{f} over the video which helps to narrow down search. This is

particularly relevant in the case of VQ2D since the task requires most recent occurrence of a query object. In Table 3, we compare performances when making “video-level” prediction by not selecting any peak and using whole video to make a prediction, v/s, making “peak-level” prediction by selecting the most recent peak. See Appendix B for more.

5. Conclusion

We present a unified approach for grounding multi-modal queries in long-form videos with different degrees of spatio-temporal outputs. To achieve that, we propose multi-task training and inference strategies that enables learning on data with varying degree of spatio-temporal annotations, and testing on variable-length, long-form videos. Finally, we observe effectiveness of our approach over task-specific

Prediction type	VQ2D			
	tAP25	stAP25	rec	Succ
Video-level	0.25	0.15	34.2	50.6
Peak-level	0.41	0.21	29.41	61.3

Table 3. **Peak-level v/s video-level predictions.** Using foreground scores to gather “regions of activity”, we choose the most recent region to form prediction (“Peak-level”) for the most recent occurrence of a query object. Compared to “Video-level” prediction which is based on whole video and does not use foreground scores, we obtain improved performance.

single architectures both in terms of performance and number of parameters.

References

- [1] Lisa Anne Hendricks, Oliver Wang, Eli Shechtman, Josef Sivic, Trevor Darrell, and Bryan Russell. Localizing moments in video with natural language. In *Proceedings of the IEEE international conference on computer vision*, pages 5803–5812, 2017. 1, 2
- [2] Taivanbat Badamdorj, Mrigank Rochan, Yang Wang, and Li Cheng. Joint visual and audio learning for video highlight detection. In *Proceedings of the IEEE/CVF International Conference on Computer Vision*, pages 8127–8137, 2021. 3
- [3] Goutam Bhat, Martin Danelljan, Luc Van Gool, and Radu Timofte. Know your surroundings: Exploiting scene information for object tracking. In *European Conference on Computer Vision*, pages 205–221. Springer, 2020. 2
- [4] Fabian Caba Heilbron, Victor Escorcia, Bernard Ghanem, and Juan Carlos Niebles. Activitynet: A large-scale video benchmark for human activity understanding. In *Proceedings of the IEEE conference on computer vision and pattern recognition*, pages 961–970, 2015. 1
- [5] Nicolas Carion, Francisco Massa, Gabriel Synnaeve, Nicolas Usunier, Alexander Kirillov, and Sergey Zagoruyko. End-to-end object detection with transformers. In *European conference on computer vision*, pages 213–229. Springer, 2020. 2, 5
- [6] Jingyuan Chen, Xinpeng Chen, Lin Ma, Zequn Jie, and Tat-Seng Chua. Temporally grounding natural sentence in video. In *Proceedings of the 2018 conference on empirical methods in natural language processing*, pages 162–171, 2018. 1, 2
- [7] Jingyuan Chen, Lin Ma, Xinpeng Chen, Zequn Jie, and Jiebo Luo. Localizing natural language in videos. In *Proceedings of the AAAI Conference on Artificial Intelligence*, volume 33, pages 8175–8182, 2019. 2
- [8] Shizhe Chen, Pierre-Louis Guhur, Cordelia Schmid, and Ivan Laptev. History aware multimodal transformer for vision-and-language navigation. *Advances in Neural Information Processing Systems*, 34:5834–5847, 2021. 3
- [9] Shaoxiang Chen and Yu-Gang Jiang. Semantic proposal for activity localization in videos via sentence query. In *Proceedings of the AAAI Conference on Artificial Intelligence*, volume 33, pages 8199–8206, 2019. 2
- [10] Shoufa Chen, Peize Sun, Enze Xie, Chongjian Ge, Jiannan Wu, Lan Ma, Jiajun Shen, and Ping Luo. Watch only once: An end-to-end video action detection framework. In *Proceedings of the IEEE/CVF International Conference on Computer Vision*, pages 8178–8187, 2021. 3
- [11] Xinlei Chen, Hao Fang, Tsung-Yi Lin, Ramakrishna Vedantam, Saurabh Gupta, Piotr Dollár, and C Lawrence Zitnick. Microsoft coco captions: Data collection and evaluation server. *arXiv preprint arXiv:1504.00325*, 2015. 6
- [12] Yen-Chun Chen, Linjie Li, Licheng Yu, Ahmed El Kholy, Faisal Ahmed, Zhe Gan, Yu Cheng, and Jingjing Liu. Uniter: Universal image-text representation learning. In *European conference on computer vision*, pages 104–120. Springer, 2020. 3
- [13] CVPR. 1st Ego4D Workshop @ CVPR 2022. <https://ego4d-data.org/workshops/cvpr22/>, 2022. [Online; accessed 09-Nov-2022]. 7, 8
- [14] Karan Desai and Justin Johnson. Virtex: Learning visual representations from textual annotations. In *Proceedings of the IEEE/CVF conference on computer vision and pattern recognition*, pages 11162–11173, 2021. 3
- [15] Jiyang Gao, Chen Sun, Zhenheng Yang, and Ram Nevatia. Tall: Temporal activity localization via language query. In *Proceedings of the IEEE international conference on computer vision*, pages 5267–5275, 2017. 1, 2
- [16] Soham Ghosh, Anuva Agarwal, Zarana Parekh, and Alexander Hauptmann. Excl: Extractive clip localization using natural language descriptions. *arXiv preprint arXiv:1904.02755*, 2019. 2
- [17] Kristen Grauman, Andrew Westbury, Eugene Byrne, Zachary Chavis, Antonino Furnari, Rohit Girdhar, Jackson Hamburger, Hao Jiang, Miao Liu, Xingyu Liu, et al. Ego4d: Around the world in 3,000 hours of egocentric video. In *Proceedings of the IEEE/CVF Conference on Computer Vision and Pattern Recognition*, pages 18995–19012, 2022. 1, 2, 6, 7, 8, 13, 15
- [18] Chunhui Gu, Chen Sun, David A Ross, Carl Vondrick, Caroline Pantofaru, Yeqing Li, Sudheendra Vijayanarasimhan, George Toderici, Susanna Ricco, Rahul Sukthankar, et al. Ava: A video dataset of spatio-temporally localized atomic visual actions. In *Proceedings of the IEEE Conference on Computer Vision and Pattern Recognition*, pages 6047–6056, 2018. 1
- [19] Dongliang He, Xiang Zhao, Jizhou Huang, Fu Li, Xiao Liu, and Shilei Wen. Read, watch, and move: Reinforcement learning for temporally grounding natural language descriptions in videos. In *Proceedings of the AAAI Conference on Artificial Intelligence*, volume 33, pages 8393–8400, 2019. 2
- [20] Kaiming He, Xiangyu Zhang, Shaoqing Ren, and Jian Sun. Deep residual learning for image recognition. In *Proceedings of the IEEE conference on computer vision and pattern recognition*, pages 770–778, 2016. 6
- [21] Rui Hou, Chen Chen, and Mubarak Shah. Tube convolutional neural network (t-cnn) for action detection in videos. In *Proceedings of the IEEE international conference on computer vision*, pages 5822–5831, 2017. 3
- [22] Zhijian Hou, Wanjun Zhong, Lei Ji, Difei Gao, Kun Yan, Wing-Kwong Chan, Chong-Wah Ngo, Zheng Shou, and Nan

- Duan. Cone: An efficient coarse-to-fine alignment framework for long video temporal grounding. *arXiv preprint arXiv:2209.10918*, 2022. 2
- [23] Andrew Jaegle, Sebastian Borgeaud, Jean-Baptiste Alayrac, Carl Doersch, Catalin Ionescu, David Ding, Skanda Koppula, Daniel Zoran, Andrew Brock, Evan Shelhamer, et al. Perceiver io: A general architecture for structured inputs & outputs. *arXiv preprint arXiv:2107.14795*, 2021. 2
- [24] Mihir Jain, Jan Van Gemert, Hervé Jégou, Patrick Bouthemy, and Cees GM Snoek. Action localization with tubelets from motion. In *Proceedings of the IEEE conference on computer vision and pattern recognition*, pages 740–747, 2014. 3
- [25] Aishwarya Kamath, Mannat Singh, Yann LeCun, Gabriel Synnaeve, Ishan Misra, and Nicolas Carion. Mdetr-modulated detection for end-to-end multi-modal understanding. In *Proceedings of the IEEE/CVF International Conference on Computer Vision*, pages 1780–1790, 2021. 3, 6
- [26] Will Kay, Joao Carreira, Karen Simonyan, Brian Zhang, Chloe Hillier, Sudheendra Vijayanarasimhan, Fabio Viola, Tim Green, Trevor Back, Paul Natsev, et al. The kinetics human action video dataset. *arXiv preprint arXiv:1705.06950*, 2017. 1
- [27] Wonjae Kim, Bokyung Son, and Ildoo Kim. Vilt: Vision-and-language transformer without convolution or region supervision. In *International Conference on Machine Learning*, pages 5583–5594. PMLR, 2021. 3
- [28] Ranjay Krishna, Yuke Zhu, Oliver Groth, Justin Johnson, Kenji Hata, Joshua Kravitz, Stephanie Chen, Yannis Kalantidis, Li-Jia Li, David A Shamma, et al. Visual genome: Connecting language and vision using crowdsourced dense image annotations. *International journal of computer vision*, 123(1):32–73, 2017. 6
- [29] Jie Lei, Tamara L Berg, and Mohit Bansal. Detecting moments and highlights in videos via natural language queries. *Advances in Neural Information Processing Systems*, 34:11846–11858, 2021. 1, 2
- [30] Dong Li, Zhaofan Qiu, Qi Dai, Ting Yao, and Tao Mei. Recurrent tubelet proposal and recognition networks for action detection. In *Proceedings of the European conference on computer vision (ECCV)*, pages 303–318, 2018. 3
- [31] Gen Li, Nan Duan, Yuejian Fang, Ming Gong, and Daxin Jiang. Unicoder-vl: A universal encoder for vision and language by cross-modal pre-training. In *Proceedings of the AAAI Conference on Artificial Intelligence*, volume 34, pages 11336–11344, 2020. 3
- [32] Xiujun Li, Xi Yin, Chunyuan Li, Pengchuan Zhang, Xiaowei Hu, Lei Zhang, Lijuan Wang, Houdong Hu, Li Dong, Furu Wei, et al. Oscar: Object-semantics aligned pre-training for vision-language tasks. In *European Conference on Computer Vision*, pages 121–137. Springer, 2020. 3
- [33] Yixuan Li, Zixu Wang, Limin Wang, and Gangshan Wu. Actions as moving points. In *European Conference on Computer Vision*, pages 68–84. Springer, 2020. 3
- [34] Kevin Qinghong Lin, Alex Jinpeng Wang, Mattia Soldan, Michael Wray, Rui Yan, Eric Zhongcong Xu, Difei Gao, Rongcheng Tu, Wenzhe Zhao, Weijie Kong, et al. Egocentric video-language pretraining. *arXiv preprint arXiv:2206.01670*, 2022. 7, 8
- [35] Zhijie Lin, Zhou Zhao, Zhu Zhang, Qi Wang, and Huasheng Liu. Weakly-supervised video moment retrieval via semantic completion network. In *Proceedings of the AAAI Conference on Artificial Intelligence*, volume 34, pages 11539–11546, 2020. 2
- [36] Naiyuan Liu, Xiaohan Wang, Xiaobo Li, Yi Yang, and Yueting Zhuang. Reler@ zju-alibaba submission to the ego4d natural language queries challenge 2022. *arXiv preprint arXiv:2207.00383*, 2022. 7, 8
- [37] Ye Liu, Siyuan Li, Yang Wu, Chang-Wen Chen, Ying Shan, and Xiaohu Qie. Umt: Unified multi-modal transformers for joint video moment retrieval and highlight detection. In *Proceedings of the IEEE/CVF Conference on Computer Vision and Pattern Recognition*, pages 3042–3051, 2022. 3
- [38] Yinhan Liu, Myle Ott, Naman Goyal, Jingfei Du, Mandar Joshi, Danqi Chen, Omer Levy, Mike Lewis, Luke Zettlemoyer, and Veselin Stoyanov. Roberta: A robustly optimized bert pretraining approach. *arXiv preprint arXiv:1907.11692*, 2019. 6
- [39] Jiasen Lu, Dhruv Batra, Devi Parikh, and Stefan Lee. Vilbert: Pretraining task-agnostic visiolinguistic representations for vision-and-language tasks. *Advances in neural information processing systems*, 32, 2019. 3
- [40] Jiasen Lu, Vedanuj Goswami, Marcus Rohrbach, Devi Parikh, and Stefan Lee. 12-in-1: Multi-task vision and language representation learning. In *Proceedings of the IEEE/CVF Conference on Computer Vision and Pattern Recognition*, pages 10437–10446, 2020. 2, 3, 6, 7
- [41] Niluthpol Chowdhury Mithun, Sujoy Paul, and Amit K Roy-Chowdhury. Weakly supervised video moment retrieval from text queries. In *Proceedings of the IEEE/CVF Conference on Computer Vision and Pattern Recognition*, pages 11592–11601, 2019. 2
- [42] Duy-Kien Nguyen and Takayuki Okatani. Multi-task learning of hierarchical vision-language representation. In *Proceedings of the IEEE/CVF Conference on Computer Vision and Pattern Recognition*, pages 10492–10501, 2019. 3
- [43] Junting Pan, Siyu Chen, Mike Zheng Shou, Yu Liu, Jing Shao, and Hongsheng Li. Actor-context-actor relation network for spatio-temporal action localization. In *Proceedings of the IEEE/CVF Conference on Computer Vision and Pattern Recognition*, pages 464–474, 2021. 3
- [44] Xiaojiang Peng and Cordelia Schmid. Multi-region two-stream r-cnn for action detection. In *European conference on computer vision*, pages 744–759. Springer, 2016. 3
- [45] Bryan A Plummer, Liwei Wang, Chris M Cervantes, Juan C Caicedo, Julia Hockenmaier, and Svetlana Lazebnik. Flickr30k entities: Collecting region-to-phrase correspondences for richer image-to-sentence models. In *Proceedings of the IEEE international conference on computer vision*, pages 2641–2649, 2015. 6
- [46] Subhojeet Pramanik, Priyanka Agrawal, and Aman Hussain. Omninet: A unified architecture for multi-modal multi-task learning. *arXiv preprint arXiv:1907.07804*, 2019. 3
- [47] Michaela Regneri, Marcus Rohrbach, Dominikus Wetzels, Stefan Thater, Bernt Schiele, and Manfred Pinkal. Grounding action descriptions in videos. *Transactions of the Association for Computational Linguistics*, 1:25–36, 2013. 1

- [48] Shaoqing Ren, Kaiming He, Ross Girshick, and Jian Sun. Faster r-cnn: Towards real-time object detection with region proposal networks. *Advances in neural information processing systems*, 28, 2015. 2, 13
- [49] Cristian Rodriguez, Edison Marrese-Taylor, Fatemeh Sadat Saleh, Hongdong Li, and Stephen Gould. Proposal-free temporal moment localization of a natural-language query in video using guided attention. In *Proceedings of the IEEE/CVF Winter Conference on Applications of Computer Vision*, pages 2464–2473, 2020. 2
- [50] Suman Saha, Gurkirt Singh, Michael Sapienza, Philip HS Torr, and Fabio Cuzzolin. Deep learning for detecting multiple space-time action tubes in videos. *arXiv preprint arXiv:1608.01529*, 2016. 3
- [51] Gunnar A Sigurdsson, Gül Varol, Xiaolong Wang, Ali Farhadi, Ivan Laptev, and Abhinav Gupta. Hollywood in homes: Crowdsourcing data collection for activity understanding. In *European Conference on Computer Vision*, pages 510–526. Springer, 2016. 1
- [52] Gurkirt Singh, Suman Saha, Michael Sapienza, Philip HS Torr, and Fabio Cuzzolin. Online real-time multiple spatiotemporal action localisation and prediction. In *Proceedings of the IEEE International Conference on Computer Vision*, pages 3637–3646, 2017. 3
- [53] Mattia Soldan, Mengmeng Xu, Sisi Qu, Jesper Tegner, and Bernard Ghanem. Vlg-net: Video-language graph matching network for video grounding. In *Proceedings of the IEEE/CVF International Conference on Computer Vision*, pages 3224–3234, 2021. 2
- [54] Weijie Su, Xizhou Zhu, Yue Cao, Bin Li, Lewei Lu, Furu Wei, and Jifeng Dai. Vi-bert: Pre-training of generic visual-linguistic representations. *arXiv preprint arXiv:1908.08530*, 2019. 3
- [55] Hao Tan and Mohit Bansal. Lxmert: Learning cross-modality encoder representations from transformers. *arXiv preprint arXiv:1908.07490*, 2019. 3
- [56] Jiajun Tang, Jin Xia, Xinzhi Mu, Bo Pang, and Cewu Lu. Asynchronous interaction aggregation for action detection. In *European Conference on Computer Vision*, pages 71–87. Springer, 2020. 3
- [57] Du Tran and Junsong Yuan. Max-margin structured output regression for spatio-temporal action localization. *Advances in neural information processing systems*, 25, 2012. 3
- [58] Jingwen Wang, Lin Ma, and Wenhao Jiang. Temporally grounding language queries in videos by contextual boundary-aware prediction. In *Proceedings of the AAAI Conference on Artificial Intelligence*, volume 34, pages 12168–12175, 2020. 2
- [59] Weining Wang, Yan Huang, and Liang Wang. Language-driven temporal activity localization: A semantic matching reinforcement learning model. In *Proceedings of the IEEE/CVF conference on computer vision and pattern recognition*, pages 334–343, 2019. 2
- [60] Philippe Weinzaepfel, Zaid Harchaoui, and Cordelia Schmid. Learning to track for spatio-temporal action localization. In *Proceedings of the IEEE international conference on computer vision*, pages 3164–3172, 2015. 3
- [61] Huijuan Xu, Kun He, Bryan A Plummer, Leonid Sigal, Stan Sclaroff, and Kate Saenko. Multilevel language and vision integration for text-to-clip retrieval. In *Proceedings of the AAAI Conference on Artificial Intelligence*, volume 33, pages 9062–9069, 2019. 2
- [62] Mengmeng Xu, Cheng-Yang Fu, Yanghao Li, Bernard Ghanem, Juan-Manuel Perez-Rua, and Tao Xiang. Negative frames matter in egocentric visual query 2d localization. *arXiv preprint arXiv:2208.01949*, 2022. 2, 7, 8
- [63] Antoine Yang, Antoine Miech, Josef Sivic, Ivan Laptev, and Cordelia Schmid. Tubedetr: Spatio-temporal video grounding with transformers. In *Proceedings of the IEEE/CVF Conference on Computer Vision and Pattern Recognition*, pages 16442–16453, 2022. 2, 3, 4, 5, 6
- [64] Xitong Yang, Xiaodong Yang, Ming-Yu Liu, Fanyi Xiao, Larry S Davis, and Jan Kautz. Step: Spatio-temporal progressive learning for video action detection. In *Proceedings of the IEEE/CVF Conference on Computer Vision and Pattern Recognition*, pages 264–272, 2019. 3
- [65] Qinghao Ye, Xiyue Shen, Yuan Gao, Zirui Wang, Qi Bi, Ping Li, and Guang Yang. Temporal cue guided video highlight detection with low-rank audio-visual fusion. In *Proceedings of the IEEE/CVF International Conference on Computer Vision*, pages 7950–7959, 2021. 3
- [66] Yitian Yuan, Tao Mei, and Wenwu Zhu. To find where you talk: Temporal sentence localization in video with attention based location regression. In *Proceedings of the AAAI Conference on Artificial Intelligence*, volume 33, pages 9159–9166, 2019. 2
- [67] Hao Zhang, Aixin Sun, Wei Jing, and Joey Tianyi Zhou. Span-based localizing network for natural language video localization. *arXiv preprint arXiv:2004.13931*, 2020. 2, 8
- [68] Songyang Zhang, Houwen Peng, Jianlong Fu, and Jiebo Luo. Learning 2d temporal adjacent networks for moment localization with natural language. In *Proceedings of the AAAI Conference on Artificial Intelligence*, volume 34, pages 12870–12877, 2020. 2
- [69] Zhu Zhang, Zhou Zhao, Yang Zhao, Qi Wang, Huasheng Liu, and Lianli Gao. Where does it exist: Spatio-temporal video grounding for multi-form sentences. In *Proceedings of the IEEE/CVF Conference on Computer Vision and Pattern Recognition*, pages 10668–10677, 2020. 1
- [70] Chen Zhao, Ali K Thabet, and Bernard Ghanem. Video self-stitching graph network for temporal action localization. In *Proceedings of the IEEE/CVF International Conference on Computer Vision*, pages 13658–13667, 2021. 8
- [71] Jiaojiao Zhao and Cees GM Snoek. Dance with flow: Two-in-one stream action detection. In *Proceedings of the IEEE/CVF Conference on Computer Vision and Pattern Recognition*, pages 9935–9944, 2019. 3
- [72] Jiaojiao Zhao, Yanyi Zhang, Xinyu Li, Hao Chen, Bing Shuai, Mingze Xu, Chunhui Liu, Kaustav Kundu, Yuanjun Xiong, Davide Modolo, et al. Tuber: Tubelet transformer for video action detection. In *Proceedings of the IEEE/CVF Conference on Computer Vision and Pattern Recognition*, pages 13598–13607, 2022. 3
- [73] Yue Zhao, Yuanjun Xiong, Limin Wang, Zhirong Wu, Xiaoou Tang, and Dahua Lin. Temporal action detection with

structured segment networks. In *Proceedings of the IEEE International Conference on Computer Vision*, pages 2914–2923, 2017. [1](#)

A. Implementation details

Identification of peaks. With reference to Figure 3, during inference, we choose peaks by simple thresholding over the foreground scores $\hat{\mathbf{f}} \in \mathbb{R}^T$, where T is the number of frames in a video. Following [17], we first apply a median filter, `medfilt`¹, with kernel size of 5. For VQ2D, we select the peaks with scores above 0.5 threshold and pick the latest peak among them.

For MQ and NLQ, since we need to retrieve multiple predictions, we select all the peaks above 0.1 threshold (maximum 1000 in total), and rank them according to their scores.

Forming predictions from peaks. As mentioned in Section 3.2.1, upon the selection of the peak(s), we form predictions by sampling a window size of w frames centered around every peak, and predict start and end frame, \hat{s} and \hat{e} , by considering only the predictions within the window. We do this by masking out logits $\hat{\tau}_s$ and $\hat{\tau}_e$ outside the window. We then form start and end probabilities, $\hat{\mathbf{p}}_s, \hat{\mathbf{p}}_e \in \mathbb{R}^w$ specific to the window by taking `softmax`, and picking \hat{s}, \hat{e} by taking `argmax` over the joint probability such that $\hat{e} > \hat{s}$.

For VQ2D, we choose a window of size 70 frames centered around the chosen peak to form prediction. For NLQ and MQ, we perform *test-time augmentation* by accumulating predictions at different frames-per-second (fps) to capture longer extents. For NLQ, we accumulate at fps $\{1, 5\}$, and for MQ, we accumulate at fps: $\{0.2, 0.5, 1, 1.66, 5\}$, which we empirically found to perform best for validation set. We use NMS [48] with threshold 0.4 to disambiguate repeated entries.

Implementation details. In addition to the implementation details discussed in Section 4, we use AdamW as the optimizer with learning rate for visual backbone as $1e^{-5}$, text encoder $5e^{-5}$ and the remaining components $5e^{-5}$. We train models for 25 epochs with learning rate drop by a factor of 10 at every 10^{th} epoch.

B. Ablations

Batch-level sampling: Round Robin v/s Concat. As mentioned in the main paper. Please find the Table 4 comparing *Round-Robin* and *Concat* sampling strategies.

Query embedding: Modality-specific v/s Single. In the main paper, we discussed having modality-specific query embeddings: $\mathbf{e}^{visual}, \mathbf{e}^{text} \in \mathbb{R}^d$. We also experiment with having only a single query embedding for both the modalities and compare them in Table 5. We found that,

¹<https://docs.scipy.org/doc/scipy/reference/generated/scipy.signal.medfilt.html>

across majority of the metrics in the three tasks, modality-specific query embedding performs better than the single query counterpart.

Query embedding for MQ. For MQ, the queries belong to a set of 130 activity classes, therefore, in addition to training a language encoder for embedding “*When did I do <activity c>?*”, we also experimented with *one-hot* embeddings of 130 activity classes using 1-layered MLP. Table 6 shows the results. In particular, we find that having a text encoder embed activity queries and trained along with the task results in better performance, which could result from text embeddings accounting for semantic relations among the classes.

	Methods	MQ			
		tIoU=0.3		tIoU=0.5	
		R@1x	R@5x	R@1x	R@5x
Single-Task	w/ one-hot encoding	27.30	49.27	18.22	34.54
	w/ text encoder	33.64	55.38	23.86	39.48

Table 6. MQ embedding: text encoder v/s one-hot.

MQ: fps 5 v/s fps 1. We mentioned earlier that we train using fps 5 for VQ2D and fps 1 for NLQ and MQ. We show results for fps 5 on MQ in Table 7. We found fps 1 to perform better, especially for MQ, since lower fps enables capturing longer temporal extents during training, and out of the three tasks MQ has the longest ground truth temporal extents, followed by NLQ and then VQ2D.

	Methods	MQ			
		tIoU=0.3		tIoU=0.5	
		R@1x	R@5x	R@1x	R@5x
Single-Task	fps 5	17.55	40.82	12.12	28.49
	fps 1	33.64	55.38	23.86	39.48

Table 7. MQ: fps 5 v/s fps 1.

MQ: step size of rolling windows. During evaluation, we accumulate predictions on long videos in a rolling-window fashion, where a window of size w frames is used to gather predictions with step size of k_{step} frames. In case of overlap between consecutive windows (or $k_{step} < w$), we average the predictions, $[\hat{\mathbf{b}}, \hat{\tau}_s, \hat{\tau}_e, \hat{\mathbf{f}}] \in \mathbb{R}^{T \times T}$, across overlapping frames. We show how different step size k_{step} affects performance in Table 8. In general, accumulating prediction with lower step size leads to better performance.

Strategy	VQ2D				NLQ				MQ			
	tAP25	stAP25	rec	Succ	tIoU=0.3		tIoU=0.5		tIoU=0.3		tIoU=0.5	
					R@1	R@5	R@1	R@5	R@1x	R@5x	R@1x	R@5x
Concat	0.41	0.20	27.1	59.3	6.20	17.86	3.98	10.92	31.54	53.51	21.97	39.64
Round-Robin	0.41	0.19	26.4	60.2	7.56	20.06	4.62	11.80	33.28	54.93	24.09	40.27

Table 4. **Sampling strategy for multi-task learning.** We train our All-Tasks (AT) approach using different sampling strategies and evaluated on validation set. We found that training on a concatenation of datasets (*Concat*) from the three tasks underperforms on NLQ and MQ compared to *Round-Robin* sampling.

	Methods	VQ2D				NLQ				MQ			
		tAP25	stAP25	rec	Succ	tIoU=0.3		tIoU=0.5		tIoU=0.3		tIoU=0.5	
						R@1	R@5	R@1	R@5	R@1x	R@5x	R@1x	R@5x
All-Tasks	single query	0.40	0.18	25.9	58.7	7.92	19.23	5.21	11.95	32.89	55.98	24.39	42.04
	multi-modal query	0.41	0.19	26.4	60.2	7.74	21.14	4.78	12.60	34.82	56.68	25.58	42.30
	query												

Table 5. **All-Tasks model using multi-modal query v/s single query embedding.** We found that on majority of performance metrics across all the tasks, multi-modal query embedding (*visual* and *textual* components) performs better than having a single query embedding.

	Step size k_{step}	MQ			
		tIoU=0.3		tIoU=0.5	
		R@1x	R@5x	R@1x	R@5x
All-Tasks	200	30.49	51.93	20.01	37.31
	100	33.28	54.93	24.09	40.27
	50	34.82	56.68	25.58	42.49

Table 8. **MQ: Effect of step size k_{step} during evaluation.**

C. Additional results

Qualitative video results. We provide video predictions in the Supplementary zip file. After extracting, please find

the files: `vq2d.mp4`, `nlq.mp4`, `mq.mp4` corresponding to VQ2D, NLQ and MQ respectively. We show a few example predictions for each of the tasks, with parts of the videos sped up with no ground-truth and predictions.

Pair-wise joint training results. In Table 9, we show all pair-wise joint training results on validation set.

		VQ2D				NLQ				MQ				# params (# models)
		tAP ₂₅	stAP ₂₅	rec%	Succ	tIoU=0.3		tIoU=0.5		tIoU=0.3		tIoU=0.5		
						R@1	R@5	R@1	R@5	R@1x	R@5x	R@1x	R@5x	
Joint	1 Ego4D [17]	0.20	0.12	32.2	39.8	5.45	10.74	3.12	6.63	33.45	58.43	25.16	46.18	
	2 Single-Task	0.41	0.21	29.4	61.2	6.53	17.22	3.61	9.58	33.64	55.38	23.86	39.48	432M (3)
	3 MQ + NLQ	-	-	-	-	7.72	19.80	4.75	11.82	32.68	54.16	24.27	41.41	185M (1)
	4 MQ + VQ2D	0.41	0.20	27.7	60.2	-	-	-	-	33.87	56.35	25.47	42.32	186M (1)
	5 NLQ + VQ2D	0.40	0.19	27.7	60.0	6.17	16.86	3.67	10.12	-	-	-	-	186M (1)
	6 All-Tasks (AT)	0.41	0.19	26.4	60.2	7.74	21.14	4.78	12.60	34.82	56.68	25.58	42.30	186M (1)

Table 9. **Pair-wise joint training results on validation set.** We observe that typically, the pair-wise joint models perform better than *Single-Task* models.